Creep Damage Calculation for Thermo Mechanical Fatigue. Case Study: Thermo Mechanical Loading in Bevelled Area between Two Cylindrical Shells with Different Thicknesses[1]

PARASCHIVA BUSUIOCEANU (GRIGORIE)[1]
STEFANESCU MARIANA-FLORENTINA [2]

1 PhD Candidate, Teacher, Viilor Economic College Viilor, Bucharest, Romania and Orthodox Theological Seminary, Bucharest
[2]Deputy Dean Faculty of Mechanical Engineering and Mechatronics, PhD. Eng. Politehnica University of Bucharest

Abstract
*The models of **thermomechanical fatigue** life prediction used for superalloys can be classified into five types: general damage models, damage-rate models, thermomechanical fatigue/strain-range partitioning methods, modified J-integral models, and empirical models. The formulation, which simulates the damage mechanisms and predicts the thermomechanical fatigue lives in various models, has been specified. However, in-depth understanding and theoretical modeling of thermomechanical fatigue damage mechanisms and interactions are still lacking[**1**]. Based on the evaluated intensity of the stress, it can be concluded which is the preferred variant the design stage, or deduction of the same sizes, in case of technological deviations (cutting errors, so as to result the same inner or outer surface, as in case of the same median surface). Article content refers in this configuration the setting mode related of connection loads that will be taken into account in tensions **[5].***

[1] This work was partially supported by the strategic grant POSDRU/159/1.5/S/137070 (2014) of the Ministry of National Education, Romania, co-financed by the European Social Fund – Investing in People, within the Sectoral Operational Programme Human Resources Development 2007-2013.

Keywords: creep, cylindrical shell, damage model, thermomechanical fatigue (TMF), short structural elements.

1.INTRODUCTION[1,4,5,7,8]

This paper addresses the problem of stress concentration in the transition area, between two cylindrical shells with different thicknesses. To reduce the intensity of the stresses and strains developed under the action of external mechanical and /or thermal loads, an original method is proposed, using method of short structural elements for shells, respectively bending moments theory and deformations continuity (displacements and rotations). In this sense, the transition between shell rings is considered linear variable in four constructive variants (with the same inner or outer surface, respectively the same median surface, or different median surfaces)**[5].**

For the needs of the creep damage prediction of thermo mechanically loaded components, software has been developed. It enables master curve determination using the time-temperature parameters and creep damage calculation using Robinson's damage accumulation rule and simple time integration**[4].** The developed software makes it possible to calculate fatigue and creep damage, respectively. In the article the most used time-temperature parameters are introduced, a fast and user-friendly master curve determination is presented and an example of creep damage on a real set of data with a simple temperature-stress history is shown **[4].**
Automotive components, gas and steam turbines, power plants and other products that operate at high temperature are subjected to creep. The lifetime of these components depends on thermal and mechanical loading. Typical examples are start-up, full load, partial load and shut-down **[4, 6].** The creep damage can no longer be neglected when the loading temperature exceeds the creep temperature typically determined as 40% of the melting temperature of the material **[4,7]** to **[4, 8].** Thus one of the critical factors in determining the lifetime of components is also their creep resistance. Due to the thermal loads materials slowly but constantly creep even at low mechanical loading, so rupture is possible.
Rupture can be defined by some limit value of strain or by actual rupture depending on the type
of component. It can be shown that the creep damage is determined by knowing the time to rupture depending on stress level and temperature**[4].**
Thermomechanical fatigue (TMF) with or without superimposed creep is the primary life-**limiting factor**

for engineering components in many high-temperature applications. In early work, isothermal fatigue (IF) tests performed at various temperatures, **mechanical strain** ranges, and strain rates were used to estimate the life of members undergoing thermomechanical damage **[1,9,10].** A major concern has been the difficulty of simulating thermal stress cycling in the laboratory. However, isothermal tests may not capture many of the important damage micromechanisms under varying temperature conditions. Recently, considerable effort has been devoted to developing TMF tests to simulate the behavior of the materials undergoing thermomechanical fatigue. Some studies have attempted to develop TMF life-prediction methods**[1].**

In TMF tests, a specimen is subjected to a desired temperature and mechanical strain with different phasings. Two baseline TMF tests are conducted in the laboratory with proportional phasings: in-phase (IP), the maximum strain at the maximum temperature, and out-of-phase (OP), the maximum strain at the minimum temperature. The variation of thermal, mechanical, and total strain components with time in OP and IP cases is illustrated in Figure 1. These two types of phasings reproduce many of the mechanisms that develop under TMF. The mechanical strain (ε_{mech}) is the sum of the elastic and inelastic strain components, while the total strain (ε_{tot} or ε_t) is the sum of thermal and mechanical strain components

$$\varepsilon_{tot} = \varepsilon_{th} + \varepsilon_{mech} = \alpha(T-T_0) + \varepsilon_{mech} \qquad (1)$$

where ε_{th} is the thermal strain, T_0 is the reference temperature where the **test** was begun, T is the test temperature, and $\alpha$is the coefficient of thermal expansion**[1].**

A schematic of the stress-strain behavior corresponding to TMF-OP and TMF-IP cases is illustrated in Figure 2. In the TMF-OP case, the material undergoes compression at high temperatures and tension at low temperatures. The inverse behavior is observed for the TMF-IP case. The mean stress of the cycle is tensile in the TMF-OP case, while it is compressive in the TMF-IP case.

Except in the baseline TMF tests, the phasing of strain and temperature can vary to a great extent. Realistic simulation-type cycles are preferred, which often have a large hysteresis. One example is a diamond-shaped cycle (figure 3),

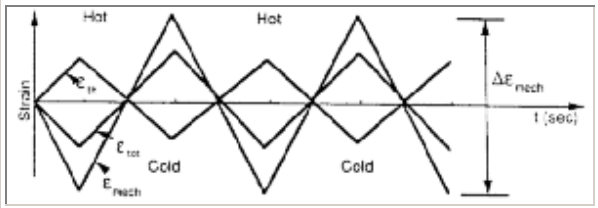

a

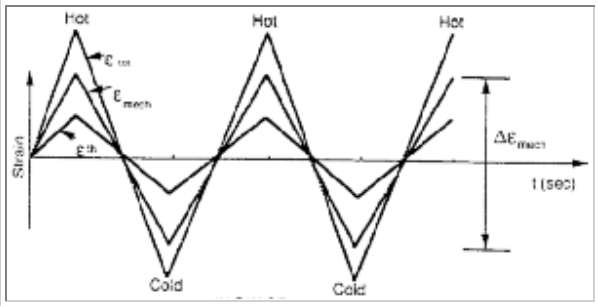

b

Figure 1. Strain versus time under **(a)** TMF-OP and **(b)** TMF-IP cases.[1,11]

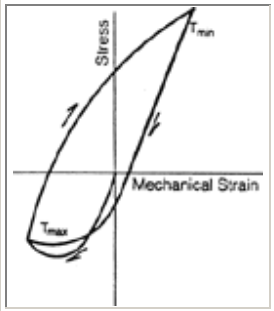

a

b

Figure 2. Stress versus strain under **(a)** TMF-OP and **(b)** TMF-IP cases. [1,9].

with the intermediate temperature being reached at the largest **tensile and compressive** strains, respectively, and the highest and lowest temperatures at zero strain.

Under TMF conditions, damage mechanisms prevalent in metals involve three major aspects: fatigue, environmental (oxidation), and creep damage. These damage mechanisms may act independently or in combination according to various materials and operating conditions, such as maximum and minimum temperatures, temperature range, mechanical strain range, strain rate, the phasing of temperature and strain, dwell time, or environmental factors.

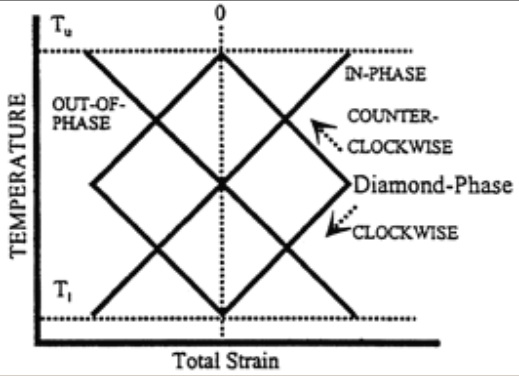

Figure 3. Temperature-strain cycles for different TMF tests (T_u—upper temperature, T_l—**low temperature**). [1,10].

$$\frac{1}{N_f} = \frac{1}{N_f^{fat}} + \frac{1}{N_f^{ox}} + \frac{1}{N_f^{creep}} \qquad (1')$$

Fatigue-Damage Term [1]

Traditionally, fatigue damage is the cyclic plasticity-driven, time- and temperature-independent damage that exists whenever cyclic loading occurs. Creep refers to a material undergoing viscous deformation at a constant stress level. This type of deformation leads to intergranular creep cavity growth and rupture. Under TMF loading, however, creep deformation contributes to the formation and propagation of microcracks. Metals exposed to environments at high temperatures are subjected to corrosion by oxidation. This kind of corrosion is accelerated by a tensile stress. During TMF, brittle oxides can enhance the nucleation and propagation of fatigue microcracks and impede the rewelding of crack surfaces during unloading.

Due to complexity, a well-accepted framework for the prediction of TMF life has been elusive. Various **approaches** have been taken, ostensibly nonisothermal generalizations of isothermally derived models.

2.GENERAL LINEAR ACCUMULATION DAMAGE MODELS[1, 9,11,12,13,14]

Neu and Sehitoglu have developed a general model for high-temperature fatigue, including thermal mechanical fatigue. This model incorporates damage accumulation due to fatigue, environment (oxidation), and creep processes. Damages per cycle from fatigue, environmental attack (oxidation), and creep are summed to obtain a total damage per cycle

$$D^{tot} = D^{fat} + D^{ox} + D^{creep} \qquad (2)$$

Assuming that linear damage is equal to one at failure, the equation may be rewritten in terms of the life, N_f, where damage is taken as equal to $1/N_f$,

Fatigue damage is represented by fatigue mechanisms, which nominally occur at ambient or low temperatures. The fatigue **life term**, N_f^{fat}, is represented by the strain-life relation

$$\frac{\Delta\varepsilon_m}{2} = C\left(2N_f^{fat}\right)^d \qquad (4)$$

where $\Delta\varepsilon_m$ is the mechanical strain range, and C and d are material constants determined from low-temperature isothermal tests[1].

Environmental-Damage (Oxidation) Term [1]

The oxidation damage is based on crack nucleation and growth through an oxide layer. It can be expressed by

$$\frac{1}{N_f^{ox}} = \left[\frac{h_{cr}\delta_0}{B\Phi^{ox}K_p^{eff}}\right]^{-\frac{1}{\beta}} \frac{2\left(\Delta\varepsilon_m\right)^{(2/\beta)+1}}{\dot{\varepsilon}^{1-(\alpha/\beta)}} \qquad (5)$$

where h_{cr} is a critical crack length at which the environmental attack trails behind the crack-tip advance, δ_0 is the ductility of the environmentally affected material, B is the coefficient, $\beta$is the exponent, and $\alpha$is the strain-rate sensitivity constant[1]. The values of all above constants are determined by experiments. Φ^{ox} is a phasing factor for **environmental damage** and is defined as

$$\Phi^{ox} = \frac{1}{t_c}\int_0^{t_c} \phi^{ox} dt \qquad (6)$$

$$\phi^{ox} = \exp\left[-\frac{1}{2}\left(\frac{(\dot{\varepsilon}_{th}/\dot{\varepsilon}_m)+1}{\xi^{ox}}\right)^2\right] \qquad (7)$$

where we talk about the ratio of thermal to mechanical strain rates, and ξ^{ox} is a constant as a measure of the relative amount of oxidation damage for different thermal strain to mechanical strain ratios and is extracted from the experiments. K_p^{eff} is a parabolic oxidation constant and can be calculated by

$$K_p^{eff} = \frac{1}{t_c}\int_0^{t_c} D_0 \exp\left(\frac{-Q}{RT(t)}\right)dt \qquad (8)$$

where T(t) is the temperature as a function of time, t_c is the cycle period, D_0 is the **diffusion coefficient** for oxidation, Q is the activation energy for oxidation, and R is the gas constant [1].

Creep-Damage Term [1]

The creep-damage term is a function of temperature, effective stress, and hydrostatic stress components, and can be expressed by

$$D^{creep} = \Phi^{creep}\int_0^{t_c} A e^{(-\Delta H/RT(t))}\left(\frac{\alpha_1\bar{\sigma}+\alpha_2\sigma_H}{K}\right)^m dt \qquad (9)$$

where is the effective stress, σ_H is the hydrostatic stress, K is the drag stress, α_1 and α_2 are scaling factors that represent the relative amount of damage occurring in tension and compression, ΔH is the activation energy for the rate-controlled creep mechanism, and A and m are material constants.

$$\Phi^{creep} = \frac{1}{t_c}\int_0^{t_c}\phi^{creep}dt \qquad (10)$$

$$\phi^{creep} = \exp\left[-\frac{1}{2}\left(\frac{(\varepsilon_{th}/\varepsilon_m)-1}{\xi^{creep}}\right)^2\right] \qquad (11)$$

the constant, ξ^{creep}, defines the sensitivity of the phasing to the creep damage.

This model couples a viscoplastic, nonisothermal constitutive model of material under investigation with an incremental evolution of damage for oxidation and creep terms within a TMF loading cycle. The model was applied to MAR-M247 and 1070 steel, and 80% of the predictions were within a factor of ± 2.5 of the experimentally measured lives**[1,9,13,16].**

3. MASTER CURVES[B+REF14,6,7,8,15]

The criterion for creep damage calculation is given by master curves which represent time to rupture depending on stress level and temperature(figure 4). Each point on a master curve represents a complete creep-rupture test at constant temperature and stress level. As expected, higher test temperatures shift master curves towards lower stress levels and shorter times to rupture.
Master curve determination at lower stress levels and lower test temperatures usually means tests of very long duration, thus as a rule master curves in these areas are determined by using parametric extrapolation methods **[4].**

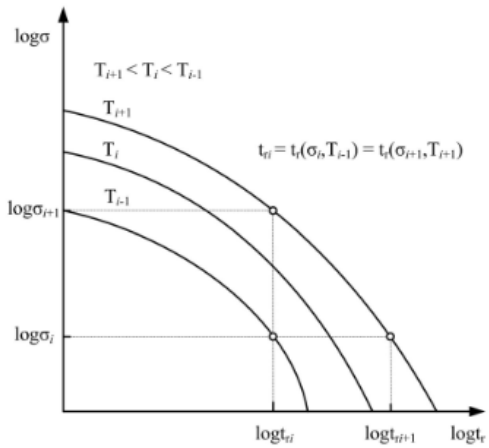

Figure 4. Master curves [**4**].

4. **CREEP DAMAGE ACCUMULATION RULE[2,5,6,7,8,15,16,17,18,19,20,21,22,23]**
Although the creep damage at controlled test conditions is relatively easy to obtain, components rarely operate under constant conditions. The most frequently used approach to creep damage assessment under variable thermo mechanical loading is to calculate the time for which the component is subjected to some loading. Robinson proposed a linear creep damage accumulation rule **[15**]:

$$D_c = \sum_{i=0}^{n_j}\sum_{j=0}^{m_{ij}}\frac{\Delta t_{rij}(\sigma_{ij},T_{ij})}{t_{rij}(\sigma_{ij},T_{ij})} \qquad (12)$$

Avoidance of deterioration risk of any mechanical structures in general, and the structure under pressure

and / or temperature, especially involves in particular, the quality of all pre-putting into operation actions and follow up normal operation. Therefore, an unavoidable conditioning is required by influences correlation imposed by conceiving (including research and design) - manufacture - transport - installation and, ultimately, maintenance **[5,16, 17].**

Lifetime of analyzed mechanical structure depends on a properly sized based on the use of some materials and certain performing technical solutions that enable judicious assessment of stresses and deformations values which are produced under the action of existing external loads and which are forecasted to be stable over time. . In the same sense, a given geometry can be capitalized at any time in order to determine the load-carrying capacity. Not only manufacturing technologies require a gradual transition (linear or fillet corner) from a thickness another of wall but also gained experience regarding attenuation of stress concentration in cylindrical and conical construction, smooth [**5,18,24**], respectively in construction with ribs **.** Reducing of stress intensity has a very favorable effect on the consumption of construction materials and exhausted energies over the life of the structure**[5].**

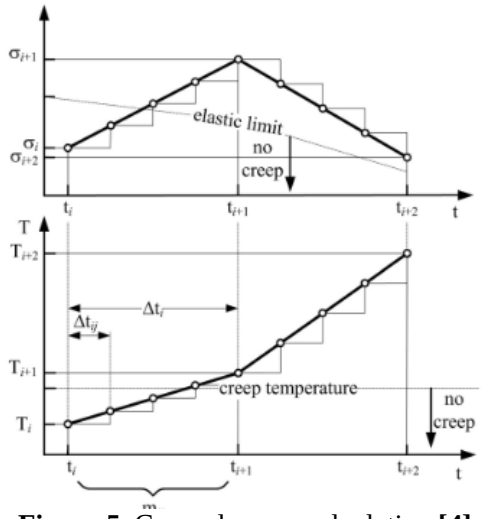

Figure 5. Creep damage calculation **[4].**

If the loading temperature is beneath the limit temperature for which material data is available, then the material data for the limit temperatures is taken into account. The damage accumulation in a single time step is independent of the previously accumulated damage. When the sum of individual creep damages reaches the defined limit value, creep rupture occurs. Robinson's damage accumulation rule is the most widely accepted one [**4,6,8,21] to [25].**

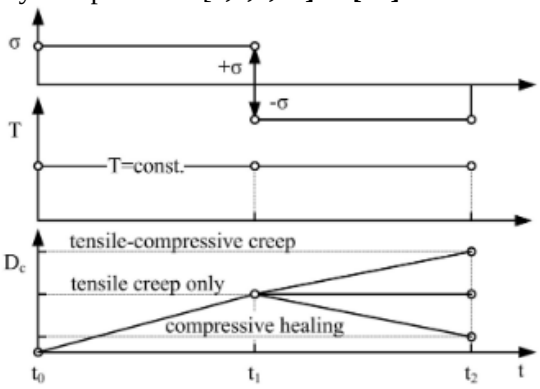

Figure 6.Influence of the creep relation upon the creep damage accumulation[**4].**

Creep damage calculation [4,8,22,23]

Creep damage is calculated as a simple integration over all the time increments according to eqation (12) (figure 5). However, there are three different creep relations used to calculate creep damage due to compressive stresses **[4,8], [4,22] and [23**].

The creep healing is possible only if Dc(t) > 0. Moreover, the tensile-compressive creep is larger than or equal to the tensile creep that is larger than or equal to the compressive healing.The appropriate creep relation depends on the material. Some materials tend to heal under compressive loading while for other materials creep damage continues to grow regardless of the direction of the loading. The influence of the creep relation on the creep damage accumulation is shown in figure 6. The temperature is supposed to be constant, while stress changes from tension to compression at t1. Before t1 the creep relation does not affect Dc. However, after t1 the tensile-compressive creep results in the highest Dc, while compressive healing in the lowest**.[4]**

5. CASE STUDY: THERMO MECHANICAL LOADING IN BEVELLED AREA BETWEEN TWO CYLINDRICAL SHELLS WITH DIFFERENT THICKNESSES [5,18,19.20.24]. This paper aims to present an original methodology based on the theory of unitary bending moments, characteristic for shells of revolution, respectively shorter structural theory. In this sense it pursues, to the present case, the determination of related loads

(unitary radial bending moments, cutting efforts) in the separation plans of the structure elements, with transition areas from one thickness to another, with linear variation (the four cases analyzed). Their values can be used in subsequent works, at the evaluation of the average radial and annular stress, respectively of the maximal equivalent stress. Based on its value it can be concluded if the structure is

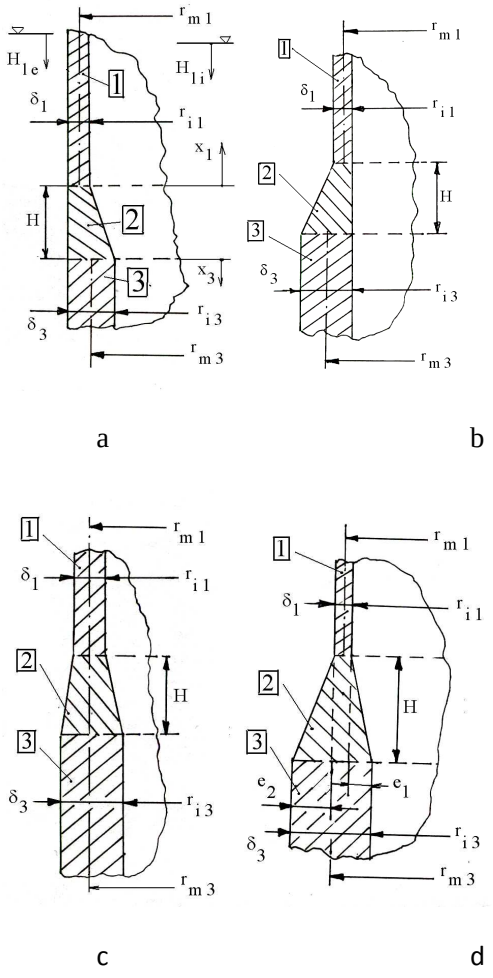

Figure 7. Types of beveled zones between two successive cylindrical shells with different thicknesses: [5]

7a - constant outer radius;7b - constant inner radius;7 c - constant median radius (symmetrical beveled area); 7d - different medial surfaces (unsymmetrical beveled area)

able to operate or it's necessary to go to specific adaptations: changing the construction material or the geometry used in the study.

An interesting observation is that the above results can be adjusted accordingly, when the switch between two different thicknesses of the shells are made through connections with identical or different geometry **[5,18,19.20.24]**.

Another paper**[5]** proposed the evaluation of loading status, in the crossing beveled zone, between two cylindrical shells with different thicknesses (Figure 7). Evaluation was performed based on the theory of bending moments, of revolution shells and of congruence deformations on the one hand, **[5],** and of method of short structural elements [19,20], on the other hand. The paper sets out how the deduction of link loads, developed under the action of considered external loads, between shells and short structural elements (type cylindrical shell with length shorter than semiwave length [5], on the one hand, and between mentioned elements [5], on the other hand. Some recognized normative [5], make adequate specifications on the geometry of such beveled zones. Practice can not meet always such recommendations, and as such it is required an atypical methodology for specific case.

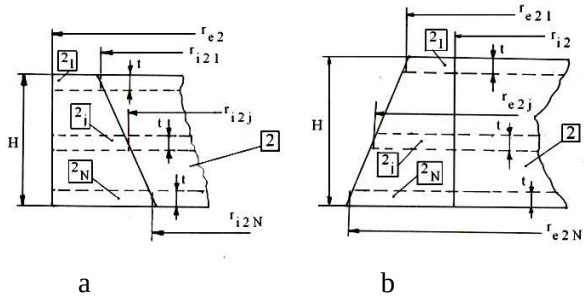

Figure 8.

8a- Dividing of beveled shape zone presented in Figure 7.a

8b- Dividing of beveled shape zone presented in Figure7.b.

In the future we will try to make creep damage calculation in this case study. For achievement of the proposed aim, beveled zones of link are divided (figure 8-10), between the two successive cylindrical shells, in any number of short cylindrical elements (blades). Considering H - the zone height of a mentioned form, the N- the number of the lamellar elements of equal height, t(it is noted that the method also allows separation with different thickness which is accepted by researcher), it is deducted:

$$t = H / N .$$

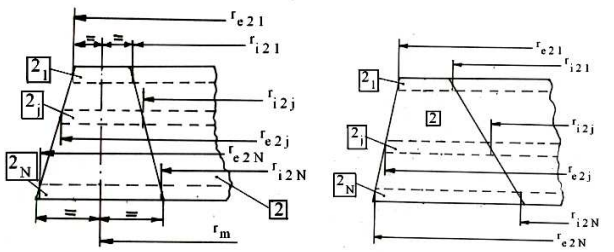

a b

Figure 9.[5]

9a-Dividing of beveled shape zone presented in figure7.c.

9b-Dividing of beveled shape zone presented in figure 7.d.

6.THE CUMULATIVE CREEP-FATIGUE DAMAGE (TMF/SRP-DAMAGE COUPLING) MODEL[4,25,29]

Most applications that involve TMF loading also include complex multilevel cyclic loading patterns, so that cumulative damage effects are also a concern. The model of cumulative creep-fatigue damage, proposed by McGaw, rests on the notion that certain basic damaging modes of cyclic deformation characterize the failure behavior of a material and utilize the SRP method as its basis[25,29].

A set of damage-curve relations is proposed for the modeling of damage accumulation according to each of the four fundamental deformation and damage modes given in SRP

$$D_{ij} = \left(\frac{n}{N_{ij}}\right)^{N_{ij}^{\alpha_{ij}}} \qquad (13)$$

where α_{ij}, i,j = p,c may be considered as material-dependent parameters, and the damage variable, D, possesses a range of 0 (undamaged condition) to 1 (failure) over the domain of the life fraction n/N_{ij} of 0 to 1.

When multiple damage modes are operative, an additional set of damage coupling relations is required,

$$D = g_{ij}\left(D_{ij}\right) \qquad (14)$$

where the functions, g_{ij}, i,j = p,c [where $g_{pp}(D_{pp}) \equiv D_{pp}$] must be determined by experiments.

The coupling relations recognize that what is considered as damage in one context cannot be necessarily regarded as damage in another (e.g., pp-type cycling is associated with transgranular, classical fatigue-type damage, while cp-type cycling is associated with intergranular, creep-type damage). However, the coupling relations do imply that the damage state is relatable. The coupling relations provide a mapping or correspondence between damage modes.

To model the more general problem wherein multiple damage modes may be present within a single cycle, one additional relationship must be established—a description of how the various damaging contributions may be synthesized to provide a means of assessing the cumulative damage contribution

$$\frac{n}{N_f} = F_{pp} D_{pp}^{N_{FF}^{-\alpha_{FF}}} + F_{cp} D_{cp}^{N_{cF}^{-\alpha_{cF}}} + F_{pc} D_{pc}^{N_{Fc}^{-\alpha_{Fc}}} + F_{cc} D_{cc}^{N_{cc}^{-\alpha_{cc}}} \qquad (15)$$

This equation describes the cumulative damage behavior of a complex cycle (with life N_f) as life fraction, expressed in terms of the four damage variables, D_{pp}, D_{cp}, D_{pc}, and D_{cc}. Note that in general, the coupling relations must be invoked to recast Equation 57 in terms of one effective damage variable, D. The model can be readily extended to treat the case of TMF through the use of the bithermal fatigue approximation to TMF[4]. To address TMF, the life relations, damage-curve equations, and damage-coupling relations can be directly replaced by bithermal counterparts. Experiments consisting of two-level loadings of TMF (both IP and OP) followed by isothermal fatigue to failure were conducted on 316 stainless steel. It was found that the model gave good predictions for the OP two-level tests and provided reasonable bounds for the IP two-level tests [4].

7. THE MODIFIED EFFECTIVE J-INTEGRAL FRACTURE MECHANICS MODEL[1,30,31,32]

A model by Nisseley was developed to predict TMF crack initiation and estimate Mode I crack growth in gas turbine hot-section gas-path superalloys. The model is based on a strain-energy-density fracture mechanics approach modified to account for thermal exposure and single-crystal anisotropy.

An effective J-integral was developed for TMF crack-life prediction. The effective J-integral is an empirical strain-energy-density crack growth parameter and is not a rigorous fracture mechanics parameter**[1,30,31,32]**.

The developed effective J-integral fracture mechanics TMF model is summarized as

$$\frac{da}{dN} = A J_{eff} \nu^c \qquad (16)$$

where a is the crack depth, da/dN is the crack-growth rate, J_{eff} is the effective J-integral (an empirical strain-energy-density fracture mechanics parameter), A and c are material constants, and

$$\frac{1}{\nu} = \int_{cycle} \exp\left[Q_0\left(\frac{1}{T_0} - \frac{1}{T}\right)\right] dt \qquad (17)$$

where Q_0 and T_0 are material constants, T is the absolute temperature, and dt is the time increment.

$$J_{eff} = \pi(a + a_0)(\beta^2 f W_{eff}^{tot})^b - J_{th} \qquad (18)$$

where a_0 is the initial material defect size (material constant), b is a material constant, β is the crack-boundary-correction factor, and J_{th} is the threshold J-integral that may be constant or temperature-dependent. For the latter, a good empirical temperature-dependent formula of J_{th} is

$$J_{th} = \begin{cases} J_0 \exp\left[Q_0\left(\frac{1}{T_{max}} - \frac{1}{T_J}\right)\right] & \text{for } T_{max} \geq T_J \\ J_0 & \text{for } T_{max} < T_J \end{cases} \qquad (19)$$

where J_0 is a constant and T_J is the temperature at which time-dependent deformation (creep) becomes significant in monotonic tensile tests.

Where f is a crystallographic strain-energy-correction factor,

$$f = f_{<111>}(E_{max} / E_{<111>})^2 \qquad (20)$$

where $f_{<111>}$ is a factor that resolves σ_{max} into the maximum normal octahedral slip plane stress, E_{max} is the elastic modulus in the σ_{max} direction and at the σ_{max} temperature, $E_{<111>}$ is elastic modulus in the <111> crystal direction and at the σ_{max} temperature, and W_{eff}^{tot} is the effective total strain-energy density.

$$W_{eff}^{tot} = 2W_e + \gamma W_p \qquad (21)$$

where γ is the material constant, and W_e is the elastic strain-energy density

$$W_e = (\sigma_{max} - m\sigma_{min})^2 / 2E_{max} \qquad (22)$$

where m = 1 if $\sigma_{min} > 0$ and m = 0 if $\sigma_{min} \leq 0$.

W_p is the plastic strain energy density:

$$W_p = \int_{cycle} \sigma d\varepsilon_{in} \qquad (23)$$

where $\sigma > 0$, σ is the stress, σ_{max} is the maximum stress, σ_{min} is the minimum stress of a cycle in which σ_{max} occurs, and $d\varepsilon_{in}$ is the inelastic strain increment**[1,30,31,32]**.

This TMF model's material constants are determined from a combination of uniaxial TMF and oxidation tests and by applying a nonlinear least-squares-regression analysis. Stresses were obtained from a nonlinear finite-element analysis of a TMF specimen strain-temperature history. Nonlinear stress-strain behavior was predicted using unified viscoplastic constitutive models.

The TMF life-model formulation is limited to transgranular cracking. The model can capture many TMF cracking effects, such as coating thickness, single-crystal anisotropy, cycle wave shape, dwell, and thermal exposure. TMF life predictions based on the modified effective J-integral model were in good agreement with observed uniaxial TMF specimen lives**[1,30,31,32]**.

9. OTHER APPROACHES [1,30,31,32,33]

Other TMF life-prediction approaches are mostly empirical models or engineering models.

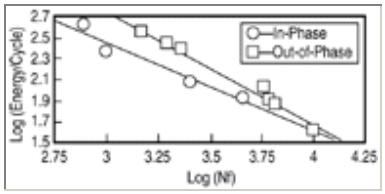

Figure 10. [1]Hysteretic energy life curves for a 316 stainless steel subjected to TMF tests in the temperature range of 399-621°C.

Bernstein and colleagues developed a model to predict the TMF life of industrial gas-turbine blades. The model is a semi-empirical approach, similar to most engineering models that are actually used to predict low-cycle fatigue. The formulation does not attempt to separately model the different mechanisms of damages (i.e., fatigue, creep, and environmental attack) **[1,30,31,32]**.

The model developed for gas-turbine blades in electric power generation is based upon the parameters of strain range, strain amplitude ratio, and dwell time. This combination of parameters is intuitively reasonable, since the strain-amplitude ratio can account for mean strain effects, and the dwell time can consider environmental and mean stress effects caused by steady-state stress relaxation, both of which can affect the fatigue life.

The general form of the model is

$$N_f = C_0(\Delta\varepsilon)^{C_1}(t_h)^{C_2}\exp\left(\frac{C_3}{A}\right) \qquad (24)$$

where N_f is the fatigue life; A is the strain ratio, A = $\varepsilon_{amp}/\varepsilon_{mean}$ (ε_{amp} = , ε_{mean} = , where all strains are mechanical strains); $\Delta\varepsilon$is the total strain range; t_h is the dwell time; and C_i (i = 0, 1, 2, and 3) is the empirical constant, determined from multiple regression of the TMF test data. In a test, the model adequately described the behavior of IN-738LC superalloy for the TMF-OP test conditions in the temperature range of 427-871°C**[1,30,31,32]**.

When the TMF model was used to predict the fatigue life of the in-service gas turbine blades, which may experience the different cycle types, a linear damage rule was used to account for the different cycle types

$$D' = \Sigma\left(\frac{N_i}{N_{if}}\right) \qquad (25)$$

where the damage ratio, D', was assumed to be one at 100% life consumed. N_i is the number of cycles of straining-type i, and N_{if} is the number of cycles to failure of type i.

Zamrik and colleagues have used the hysteretic-energy method to characterize the TMF behavior of type 316 stainless steel[32]. From the stabilized mid-life hysteresis loop, the energy per volume cycle or density can be calculated and fit to the energy-life relation by

$$\frac{\text{Energy}}{\text{Volume Cycle}} = \Delta U = \frac{W}{AL} = \int \sigma d\varepsilon = A_0(N_f)^a \qquad (26)$$

where ΔU is the energy per volume cycle, W is the work or area of the hysteresis loop, A is the specimen cross-sectional area, L is the specimen gage length, $\sigma$is the stress, $d\varepsilon$ is the strain increment, A_0 and a are constants, and N_f is the number of cycles to failure. The hysteretic energy versus life approach is illustrated in Figure 8. It can be observed that the TMF-IP hysteretic energy life line is lower than the TMF-OP line, which suggests more damage**[1,30,31,32]**.

Kanasaki and colleagues have carried out axial-strain-controlled low-cycle fatigue tests of a carbon steel in oxygenated high-temperature water under TMF-IP and TMF-OP conditions[33].Based on the assumption that the fatigue damage increased in a linear proportion to the increment of strain during cycling, a fatigue-life prediction method was proposed.

$$\frac{1}{N'} = \int_{T_{min}}^{T_{max}} \frac{1}{N(T)} \cdot \frac{dT}{T_{max} - T_{min}} \qquad (27)$$

where T_{max} and T_{min} are the maximum and minimum temperatures during TMF cycling, N(T) is the fatigue life in high-temperature water under isothermal conditions, and N' is fatigue life in high-temperature water under a TMF condition. For a carbon steel, STS410, under the conditions of DO = 1 ppm (in pure water containing 1 ppm oxygen) and $\dot{\varepsilon}$= 0.002% 1/s, N(T) was determined by the experiment

$$\frac{1}{N(T)} = \begin{cases} 8.755 \times 10^{-4} & (T \le 176°C) \\ 4.85 \times 10^{-5} T - 7.68 \times 10^{-3} & (176°C < T \le 290°C) \end{cases} \quad (28)$$

A good relationship between the predicted N'_{pred} and the experimental N'_{test} was observed**[1,30,31,32]**.

10. CONCLUSION [1,5]

This paper aims to present an original methodology based on the theory of unitary bending moments, characteristic for shells of revolution, respectively shorter structural theory. In this sense it pursues, to the present case, the determination of related loads (unitary radial bending moments, cutting efforts) in the separation plans of the structure elements, with transition areas from one thickness to another, with linear variation (the four cases analyzed). Their values can be used in subsequent works, at the evaluation of the average radial and annular stress, respectively of the maximal equivalent stress. Based on its value it can be concluded if the structure is able to operate or it's necessary to go to specific adaptations: changing the construction material or the geometry used in the study [5].

An interesting observation is that the above results can be adjusted accordingly, when the switch between two different thicknesses of the shells are made through connections with identical or different geometry [5].
The models described here was taken by [1] and it can be divided into two types:

- General models of TMF life prediction based on fundamental physical mechanisms of TMF crack initiation and propagation. Such models may be used to capture and simulate damage mechanisms and their interactions under TMF loading conditions. These models must be based on a number of test data sets of various materials, include microstructural observations and analyses, and generally couple viscoplastic constitutive models. But the forms or the sets of equations of these models are complex and not convenient in engineering applications[1].
- Engineering and empirical models, the objective of which is directed toward engineering practices and direct applications. It is for a special material that an empirical model of TMF life prediction is established. The forms of this model are a little simpler and convenient for applications, but they are not in common use among various materials[1].

Damage modeling under thermomechanical cyclic loading is still at an early stage. TMF cycling is expected to introduce a multitude of cyclic deformation and damage mechanisms in superalloys, and the influence of these damage mechanisms on the material's fatigue-crack initiation and propagation behavior is not well understood at present. No generally accepted models of TMF fatigue-life prediction are currently available[1].

It is generally recognized that three dominant damage mechanisms (fatigue, oxidation, and creep damage) may occur during TMF loading conditions. Most proposed models of TMF fatigue-life prediction attempt to capture the effects of these damage mechanisms and their interactions. It is not certain if these dominant damage mechanisms operate simultaneously, or if some of them run and others become inoperative during a special TMF loading condition[1].

There are many factors affecting TMF lives, such as materials, maximum and minimum temperatures, temperature range, strain rate, strain range, strain-temperature phase, and dwell and cycle times. There is a difficulty in that the models quantitatively simulate the interaction of damage mechanisms; at present, views on how to deal with this problem differ. Based on this and the complexity of alloys systems, TMF-life-prediction models are generally time-consuming and expensive[1].

To develop effective TMF life-prediction approaches for superalloys, more experimental work and data collection are necessary on various materials placed under TMF loading conditions[1].

Acknowledgements

The authors thank to the organizers of grant POSDRU/159/1.5/S/137070 (2014) for their support.

12. References

[1] Changan Cai, Peter K. Liaw, Mingliang Ye, and Jie Yu, Recent Developments in the Thermomechanical Fatigue Life Prediction of Superalloys, www.google.ro.

[2] Moridi A., Azadi M. , Farrahi G.H., Coating thickness and roughness effect on stress distribution of A356.0 under thermo-mechanical loadings, available online at www.sciencedirect.com, Procedia Engineering 10 (2011) p. 1372–1377.

[3] Moridi A., Azadi M. , Farrahi G.H., Numerical Simulation of Thermal Barrier Coating System under Thermo-mechanical Loadings , available online at http://www.iaeng.org/publication/WCE2011/WCE2011_pp1959-1964.pdf, p 1959-1964.

[4] Seruga D. , Fajdiga M., Nagode M., Creep Damage Calculation for Thermo Mechanical Fatigue, available online at www.google.ro, Journal of Mechanical Engineering 57(2011)5, p. 371-378.

[5] Zichil Valentin , Iatan I. Radu , Bibire Luminița , Busuioceanu (Grigorie) Paraschiva , Serban Laurențiu, Thermo - Mechanical Loading in Bevelled Area between two Cylindrical Shells with Different Thicknesses.Theoretical Study - Connection Loads, Journal of Engineering Studies and Research – Volume 20 (2014) No. 1, p 87-101.

[6] Hejwowski T, Weronski A. The effect of thermal barrier coatings on diesel engine performance. *Vacuum* 2002;**65**:427-32.

[7] Taymaz I, Cakir K, Mimaroglu A. Experimental study of effective efficiency in a ceramic coated diesel engine. *J Surf Coat Tech* 2005;**200**:1182-5.

[8] Ramu P, Saravanan CG. Effect of ZrO2-Al2O3 and SiC coating on diesel engine to study the combustion and emission characteristics. *SAE International*, Paper No. 2009-01-1435, 2009.

[9] H. Sehitoglu, "Thermo-Mechanical Fatigue Life Prediction Methods," *Advances in Fatigue Lifetime Predictive Techniques*, ASTM STP 1122 (1992), pp. 47–76.

[10] S.A. Kraft and H. Mughrabi, "Thermo-Mechanical Fatigue of the Monocrystalline Nickel-Base Superalloy CMSX-6," *Thermomechanical Fatigue Behavior of Materials*, ASTM STP 1263 (1996), pp. 27–40.

[11] R. Neu and H. Sehitoglu, "Thermo-Mechanical Fatigue, Oxidation and Creep: Part 1—Experiments," *Met. Trans. A*, 20A (1989), pp. 1755–1767.

[12] R. Neu and H. Sehitoglu, "Thermo-Mechanical Fatigue, Oxidation and Creep: Part 2-Life Prediction," *Met. Trans. A*, 20A (1989), pp. 1769–1783.

[13] H. Sehitoglu and D.A. Boismier, "Thermo-Mechanical Fatigue of Mar-M247: Part 2—Life Prediction," *J. Eng. Mat. and Tech.*, 112 (1990), pp. 80–89.

[14] Y. Kadioglu and H. Sehitoglu, "Modeling of Thermomechanical Fatigue Damage in Coated Alloys," *Thermomechanical Fatigue Behavior of Materials*, ASTM STP 1186 (1993), pp. 17–34.

[15] H. Sehitoglu and D.A. Boismier, "Thermo-Mechanical Fatigue of Mar-M247: Part 2—Life Prediction," *J. Eng. Mat. and Tech.*, 112 (1990), pp. 80–89.

[16] Iatan I. R., Sârbu L., Transportarea şi montarea utilajelor industriilor de proces, Parte I, Institutul Politehnic Bucureşti, 1991.

[17] [2] Iatan I. R., Vasilescu I., Transportarea utilajelor tehnologice agabaritice, Editura MatrixRom, Bucureşti, 2002

[18] x x x TGL 32903(09, Behälter and Apparate, Festigkeitsberechnung, Ebene kreisförmige Böden und Deckel, Oktober 1979, DDR – Standard.

[19] Iatan I. R., Cercetări teoretice şi experimentale privind construcțiile de îmbinări cu flanşe cu nervuri, Teză de doctorat, Institutul Politehnic din Bucureşti, 1979.

[20] Iatan I. R., Alămoreanu Elena, Iordan Nicoleta, Chiriță R., Calculus elements for ring neck flanges, Modelling and Optimization in the Machines Building Field, MOCM 3, University of Bacău, 1997, p. 14 – 17.

[21] Iatan I. R., Alămoreanu Elena, Iordan Nicoleta, Chiriță R., Calculus elements for ring neck flanges, Modelling and Optimization in the Machines Building

Field, MOCM 3, University of Bacău, 1997, p. 14 – 17.

[22] E. Chataigner and L. Remy, "Thermomechanical Fatigue Behavior of Coated and Bare Nickel-Based Superalloy Single Crystals," *Thermomechanical Fatigue Behavior of Materials,* ASTM STP 1263 (1996), pp. 3–25.

[23] L. Remy et al., "Fatigue Life Prediction under Thermo-Mechanical Loading in a Nickel-Base Superalloy," *Thermomechanical Fatigue Behavior of Materials,* ASTM STP 1186 (1993), pp. 3–16.

[24] Renert M., Calculul şi construcţia utilajului chimic, vol. 1, Editura Didactică şi Pedagogică, Bucureşti, 1971.

[25] J. Reuchet and L. Remy, "Fatigue Oxidation Interaction in a Superalloy-Application to Life Prediction in **High Temperature** Low Cycle Fatigue," *Met. Trans. A*, 14A (1983), pp. 141–149.

[26] Deloševič M., Petrovič D., Bižic M., Identification of the stress – strain state of a cylindrical tank with walls of variable thickness, FME Transaction, 39, 2011, p. 25 – 32

[27] Chen Zh., Yang L., Cao G., Guo W., Buckling of the axially compressed cylindrical shells with arbitrary axisymmetric thickness variation, Thin – Walled Structures, 60, 2012, p. 38 – 85

[28] Chen L., Rotter M. J., Doerich – Stavridis Cornelia, Practical calculations for uniform external pressure buckling in cylindrical shells with stepped walls, Thin – Walled Structures, 61, 2012, p. 162 – 168

[29] M.A. McGaw, "Cumulative Creep-Fatigue Damage Evolution in an Austenitic Stainless Steel," *Advances in Fatigue Lifetime Predictive Techniques,* ASTM STP 1122 (1992), pp. 84–106.

[30] D.M. Nissley, "Thermomechanical Fatigue Life Prediction in Gas Turbine Superalloys: A Fracture Mechanics Approach," *AIAA Journal*, 33 (6) (1995), pp. 1114–1120.

[31] H.L. Bernstein et al., "Prediction of Thermal-Mechanical Fatigue Life for Gas Turbine Blades in Electric Power Generation," *Thermomechanical Fatigue Behavior of Materials,* ASTM STP 1186 (1993), pp. 212–238.

[32] S.Y. Zamrik, D.C. Davis, and L.C. Firth, "Isothermal and Thermomechanical Fatigue of Type 316 Stainless Steel," *Thermomechanical Fatigue Behavior of Materials,* ASTM STP 1263 (1996), pp. 96–116.

[33] . H. Kanasaki et al., "Corrosion Fatigue Behavior and Life Prediction Method under Changing Temperature Condition," *Effects of the Environment on the Initiation of Crack Growth,* ASTM STP 1298 (1997), pp. 267–281